

Diffusion of colloids in one-dimensional light channels

C Lutz^{1,2}, M Kollmann³, P Leiderer² and C Bechinger¹

¹ 2. Physikalisches Institut, Universität Stuttgart, Pfaffenwaldring 57, 70550 Stuttgart, Germany

² Fachbereich Physik, Universität Konstanz, 78457 Konstanz, Germany

³ Dipartimento di Fisica, Viale delle Scienze, Università di Palermo, 90141 Palermo, Italy

Received 25 March 2004

Published 10 September 2004

Online at stacks.iop.org/JPhysCM/16/S4075

doi:10.1088/0953-8984/16/38/022

Abstract

Single-file diffusion (SFD), prevalent in many chemical and biological processes, refers to the one-dimensional motion of interacting particles in pores which are so narrow that the mutual passage of particles is excluded. Since the sequence of particles in such a situation remains unaffected over time t , this leads to strong deviations from normal diffusion, e.g. an increase of the particle mean-square-displacement as the square root of t . We present experimental results of the diffusive behaviour of colloidal particles in one-dimensional channels with varying particle density. The channels are realized by means of a scanning optical tweezers. Based on a new analytical approach (Kollmann 2003 *Phys. Rev. Lett.* **90** 180602) for SFD, we can predict quantitatively the long-time, diffusive behaviour from the short time density fluctuations in our systems.

1. Introduction

Transport phenomena are crucial for the understanding of many processes in physical, biological and chemical systems. Often, such processes take place in narrow pores or channels where the individual particles are not able to pass each other. The properties in such systems are described by single-file-diffusion (SFD) and several attempts have been made to describe the long-time behaviour of such systems. One of the most striking features of SFD compared to normal (i.e. Fickian) diffusion is the fact that the motion of the particles at long times takes place via a cooperative process because the displacement of a given particle over a long distance necessitates the motion of many other particles in the same direction. This correlation is reflected in the long-time behaviour of the mean square displacement $W(t)$ which has been predicted for an infinite system and for times t larger than the direct interaction time τ (i.e. the time a particle needs to move a significant fraction of the mean particle distance) to be [2–6]

$$\lim_{t \gg \tau} W(t) = F\sqrt{t} \quad (1)$$

where F is the SFD mobility.

Experimental evidence for such a behaviour became only recently possible due to the fabrication of artificial crystalline zeolitical structures which are believed to comprise an almost ideal test ground for the study of SFD. However, although some groups found SFD by using pulsed force gradient nuclear magnetic resonance (PFG-NMR) [10] and quasi-elastic neutron scattering techniques (QENS) [11], these results were partially questioned by other studies which indicate normal diffusion. This discrepancy is probably due to small deviations of the structure of the zeolites from an ideal, homogeneous nanoporous network. In addition, particle interaction across adjacent pores has been reported which would also lead to deviations from equation (1) [12, 13].

In order to rule out the above mentioned ambiguities, two different groups, Lin *et al* [14] and Wei *et al* [15] studied SFD in mesoscopic colloidal systems. In order to provide channel structures, they used topographical channels fabricated by means of photolithography. The particle positions were monitored with video microscopy and allowed to obtain the microscopic information of the system (in contrast to the PFG-NMR and QENS experiments where only ensemble averages could be measured). While Lin *et al* concentrated on the short time behaviour ($t \ll \tau$) and indeed found the expected normal diffusion, Wei *et al* confirmed for the first time unambiguously the predicted $t^{1/2}$ -behaviour at long times.

While most of the results for SFD are limited to hard-rod systems [7–9], only recently has it been demonstrated by one of us that equation (1) remains valid for colloidal and atomic systems with arbitrary interaction potentials, provided the correlation length between the particles is of finite range and collisions are associated with some energy dissipation [1]. In addition, it was shown that the SFD-mobility F can be determined by the compressibility and the short-time collective diffusion coefficient of the system. This is an interesting result, because it relates in a unique way a long-time feature, i.e. the SFD mobility, to the short-time collective diffusional properties of the system.

The purpose of this paper is to test this prediction by performing an experiment which covers both time regimes, i.e. the short-time and the long-time properties. This allows us to compare the SF mobilities F obtained at short times [1] with the results obtained at long times according to equation (1). The experiments were performed with colloidal particles but in contrast to earlier experiments we did not use topographical channels because this largely reduces the diffusion constants due to hydrodynamic interactions and thus increases the measuring times. Instead we created one-dimensional channels with scanned optical tweezers where such hydrodynamical effects are largely reduced (not absent). Our results clearly resolve the transition from normal diffusion at short times to the predicted $t^{1/2}$ long time behaviour of the MSD. We also compared the measured SFD-mobility with the corresponding value as obtained from the initial decay of the dynamic structure factor $S(q, t)$ and find good agreement with recent theoretical predictions [1].

2. Method

As a colloidal system we used a highly diluted aqueous suspension of sulphate-terminated polystyrene (PS) particles of $2.9 \mu\text{m}$ diameter with an average polydispersity below 4% (IDC). The experimental setup was composed of a silica glass cuvette with $200 \mu\text{m}$ spacing, which was connected to a standard deionization circuit [16] (see figure 1). Prior to inserting colloidal particles into the cell the water in the whole circuit was fully de-ionized (corresponding to an ionic conductivity below $0.07 \mu\text{S cm}^{-1}$). The experiments were performed at $294 \pm 0.5 \text{ K}$. When the cell was disconnected from the circuit, stable conditions during several hours were maintained. The confinement of the particles to 1D channels was achieved with an optical tweezer setup which provided a stable trapping potential for the colloids [17]. In order to

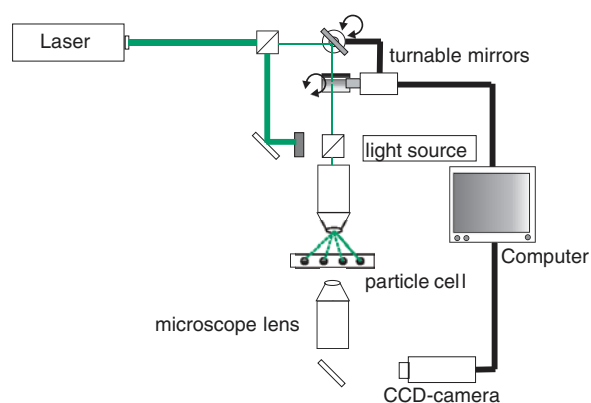


Figure 1. Schematic representation of the experimental setup.
(This figure is in colour only in the electronic version)

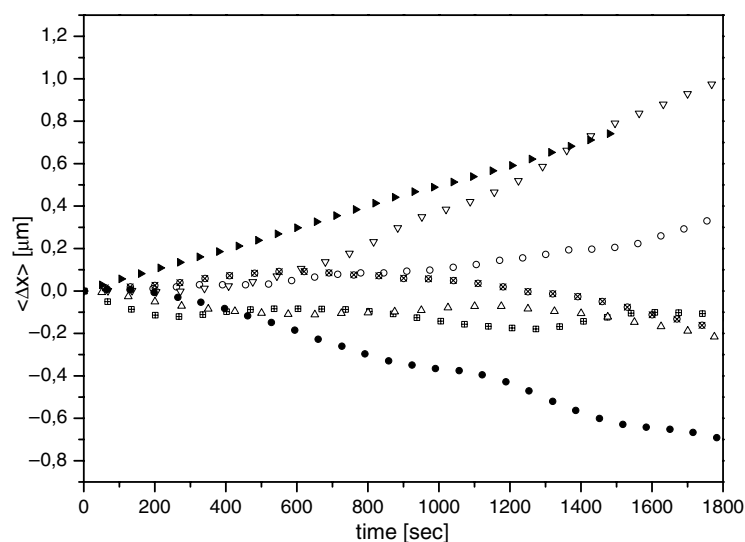


Figure 2. Average particle displacement along the circumference of the circle for different particle densities: $0.099 \mu\text{m}^{-1}$ (\otimes), $0.103 \mu\text{m}^{-1}$ (\triangle), $0.147 \mu\text{m}^{-1}$ (\blacktriangleright), $0.156 \mu\text{m}^{-1}$ (\bullet), $0.168 \mu\text{m}^{-1}$ (∇), $0.185 \mu\text{m}^{-1}$ (\circ) and $0.203 \mu\text{m}^{-1}$ (\boxplus).

create ring-shaped channel structures, a laser beam ($\lambda = 532 \text{ nm}$) was deflected from a pair of computer-controlled galvanostatic driven mirrors and focused into the sample cell where the beam created a ring-shaped light pattern. The laser was circularly polarized by a quarter-wave plate which reduced any residual inhomogeneity of the laser intensity along the circular path to about 3%. The repetition rate of the circular pattern was about 300 Hz which should be fast enough to provide a quasi-static circular optical trap for the particles [18]. To rule out any residual light-induced drifts due to the scanning laser tweezer, we calculated for all our measurements the average particle displacement $\langle \Delta x(t) \rangle$ (see figure 2) along the circle. As can be seen, the displacements are very small, not exceeding about 1/3 of a particle diameter in half an hour. In addition, the sign of $\langle \Delta x(t) \rangle$ is independent of the laser scanning direction (which was kept constant during the measurements). This rules out drift effects induced by

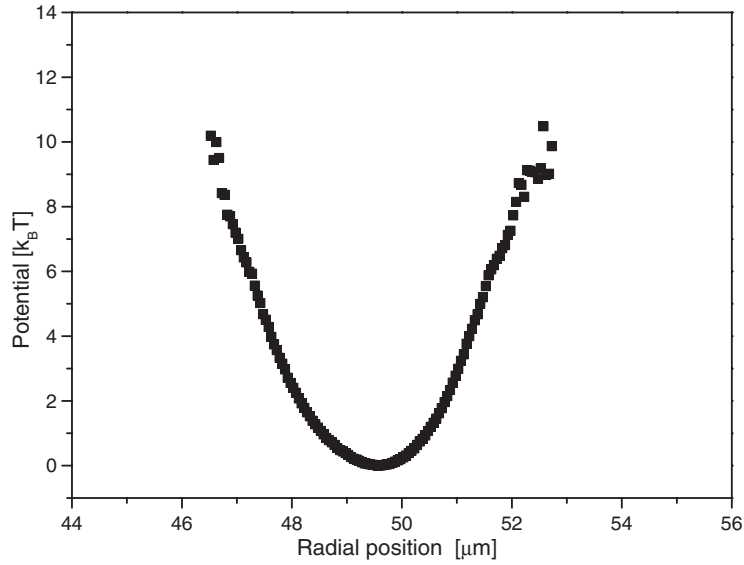


Figure 3. Example of an average light potential, perpendicular to the scanning direction, sampled by the particles due to Brownian motion.

the scanning laser beam as they were observed by other authors [18]. From a linear fit of the curves of figure 2 we obtain an averaged drift rate of about $\pm 2.9 \times 10^{-4} \mu\text{m s}^{-1}$ (this value is small compared to the effects discussed in the following). From the radial particle fluctuations we calculated via the Boltzmann statistics the radial part of the light potential as shown in figure 3. Since the half-width of the light pattern in the radial direction corresponds to about one particle diameter, the scanned-laser optical trap provided an effective 1D potential for the colloids where mutual passage of particles is excluded (under the experimental conditions radial particle fluctuations were less than one particle diameter). The depth of the light potential was of the order of $10 k_B T$ (corresponding to a laser power of 10–20 mW inside the cell), which is sufficient to impede colloidal particles from escaping out of the trap during our measuring times. Density dependent measurements were performed by variation of the radius R of the circular optical trap ($35 \mu\text{m} < R < 49 \mu\text{m}$) and the number of particles N ($22 < N < 45$).

Because the laser tweezer was incident perpendicular from above, the particles were also subjected to vertical light forces which pushed them toward the negatively charged silica substrate. Therefore the system was effectively confined to two dimensions. We estimated the effective changes in the lateral particle interaction between neighbouring particles due to the periodically pushing light forces of the rotating laser focus. A rough calculation based on [19] yields that this effect can be ignored in comparison to the static pair potential. To collect colloidal particles from the highly diluted suspensions and to insert a well-defined number into the optical circle, an additional adjustable laser tweezer was focused into the sample cell. This tweezer also served to keep diffusing particles apart from the region where the measurements were performed. The particle centre positions were analysed during the experiments online with imaging processing software, which allowed us to obtain the particle trajectories.

A typical real-space configuration of 45 particles in a circular optical trap with $R = 42 \mu\text{m}$ diameter is shown in figure 4. From the particle trajectories which were recorded up to several hours we calculated $W(t) = \frac{1}{2N} \sum_i \langle [x_i(t+t') - x_i(t')]^2 \rangle$, where x corresponds to the angular position multiplied by R , i denotes the particle index and the brackets indicate averaging over all time steps.

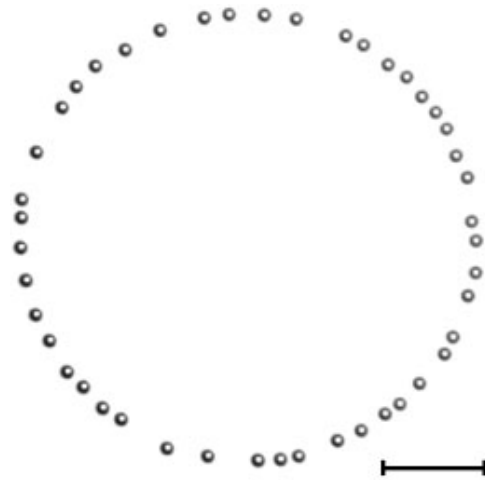


Figure 4. Image of colloidal particles which are trapped by a scanning laser beam to a circular optical trap (the trap itself is not visible but was blocked with appropriate optical filters). The bar corresponds to $20 \mu\text{m}$.

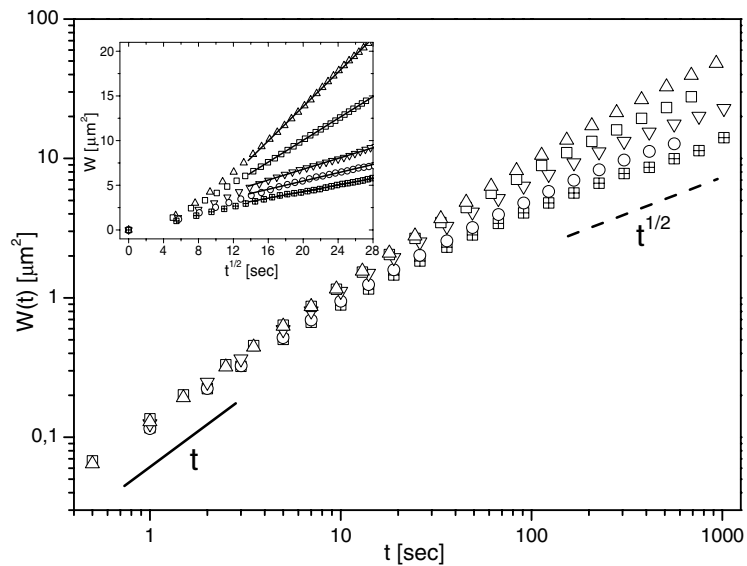


Figure 5. Double-logarithmic plot of W for $\rho = 0.103 \mu\text{m}^{-1}$ (Δ), $0.119 \mu\text{m}^{-1}$ (\square), $0.168 \mu\text{m}^{-1}$ (∇), $0.185 \mu\text{m}^{-1}$ (\circ) and $0.203 \mu\text{m}^{-1}$ (\boxplus). The solid line with slope 1 illustrates normal diffusion and the dotted line with slope 0.5 describes SFD. The inset shows the same data plotted as W versus \sqrt{t} , with the solid lines corresponding to fits to equation (1).

3. Results

The results for $W(t)$ are shown as symbols in figure 5 for different particle number densities ($\rho = 0.103 \mu\text{m}^{-1}$ (Δ), $0.119 \mu\text{m}^{-1}$ (\square), $0.168 \mu\text{m}^{-1}$ (∇), $0.185 \mu\text{m}^{-1}$ (\circ), and $0.203 \mu\text{m}^{-1}$ (\boxplus)) in a log–log representation. At sufficiently short times ($t < 10$ s), where the individual particles do not ‘feel’ the presence of other particles by direct interactions, normal diffusion

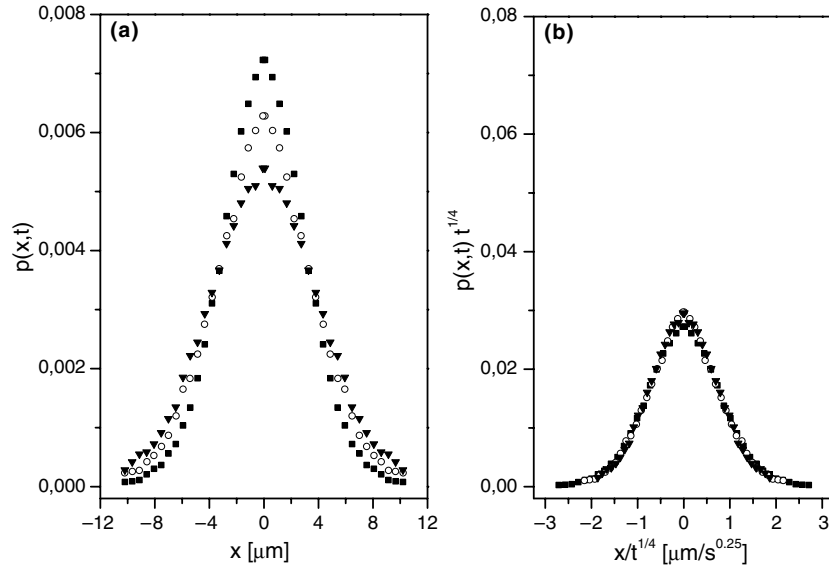


Figure 6. (a) Propagator $p(x, t)$ at four different times: $t = 201$ s (■), 501 s (○), 901 s (▼). (b) Masterplot of $p(x, t)$ after rescaling according to equation (2).

occurs and the mean square displacement is found to be $W(t) \propto t$ (see solid line). This behaviour is in good agreement with Lin *et al* who also studied the short-time diffusional motion of colloidal particles in 1D channels [14]. In the case of topographically created 1D channels, the diffusion coefficient is strongly influenced by the walls and the local particle density ρ . This dependence on hydrodynamic boundary conditions is significantly reduced in our system as lateral walls are absent and only the substrate determines the free diffusion constant. With increasing time the presence of adjacent particles becomes more and more important until eventually a crossover to a $t^{1/2}$ -behaviour occurs (dashed line in figure 5). In contrast to earlier experiments [15], here both regimes are clearly resolved for the first time. It is also seen that the crossover from normal to SFD takes place at earlier times as ρ is increased. This is due to the fact that with increasing ρ , the clearance between adjacent particles becomes smaller and therefore direct particle–particle interactions occur at shorter times. This crossover is also seen by analysing the time-dependent propagator $p(x, t)$ (see figure 6). The function is defined as the conditional probability of finding a particle at position x after time t with the particle located for $t = 0$ at $x = 0$. In the case of hard rods $p(x, t)$ has been predicted for $t \gg \tau$ to be [4, 9]

$$p(x, t) = \frac{1}{\sqrt{4\pi Ft^{1/2}}} \exp(-x^2/4Ft^{1/2}). \quad (2)$$

Figure 6(a) shows the propagator for times $t = 201$ s (■), 501 s (○) and 901 s (▼) respectively. As can be seen, $p(x, t)$ continuously decays in time. Rescaling the data according to equation (2) as $p(x, t)t^{1/4}$ versus $x/t^{1/4}$ should collapse all curves onto a single master curve. Indeed, this is in good agreement with our data (figure 6(b)).

To obtain the SFD mobility F for our data we first plotted W versus $t^{1/2}$ and applied a fit of equation (1) (see inset of figure 5). As the lower bound for the fitting range we have chosen the direct interaction time of the particles which is of the order of 200 s. It can be clearly seen, that above this time, all curves show a linear behaviour. The obtained values for F are plotted in figure 7 as solid squares and show that F decreases monotonically with ρ . Such a

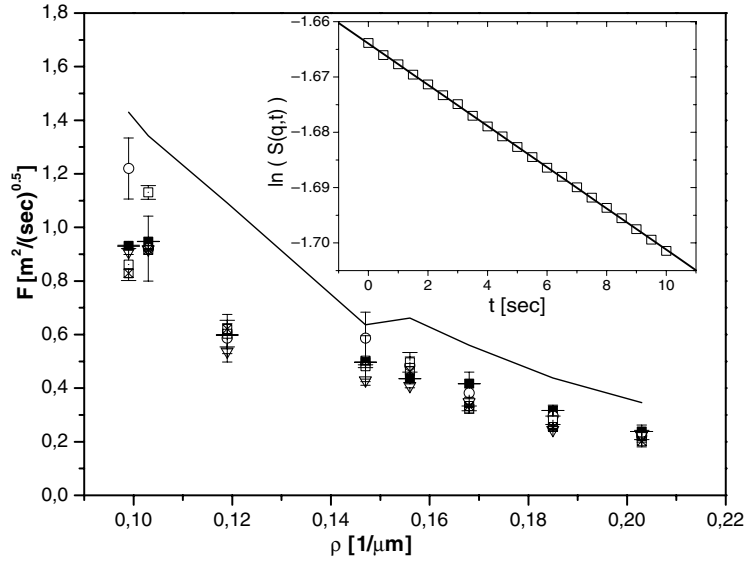


Figure 7. Comparison of SFD mobilities F obtained with different methods as a function of the particle number density ρ : F derived from fitting the MSD in figure 2 at long times (\blacksquare), F taken from the decay of the dynamic structure factor according to equation (3) for $q = 3q_{\min}$ (\circ), $q = 4q_{\min}$ (\square), $q = 5q_{\min}$ (∇), and $q = 6q_{\min}$ (\boxtimes). F taken from predictions of hard rod systems at low densities [7–9] (solid line). The inset shows the decay of $S(q, t)$ for $q = 4q_{\min}$, which follows an exponential function (solid line).

monotonic behaviour of F has also been observed for the diffusion of CF_4 in AlPO_4 -zeolites at low temperatures [3] and is in qualitative agreement with a theoretical expression derived for hard rods [6]. For comparison, we also plotted in figure 7 (solid line) the prediction for the hard rods, using the measured self-diffusion coefficient and diameter of our particles. Of course this theory does not take into account the interaction potential of the charged particles and overestimates their mobility.

It is important to realize that in the case of normal diffusion, the diffusion coefficient will saturate at small ρ while in the case of SFD, even at very low ρ , no saturation of F occurs. This emphasizes that particle–particle interactions are the limiting factor for SFD [3]. As mentioned above, theoretical predictions for the SFD mobility F were for a long time only available for hard rod systems where analytical expressions for the limit of small rod densities were derived [10]. Very recently a general theory of SFD for systems of identical Brownian particles with arbitrarily interaction potentials was developed. It has been shown [1] that the long-time behaviour of the MSD for $q \ll a^{-1}$ is given by

$$\lim_{t \gg \tau} W(t) = \frac{S(q, t=0)}{\rho} \sqrt{\frac{D^{\text{eff}}(q)t}{\pi}}. \quad (3)$$

Here $S(q, t=0)$ is the static structure factor and $D^{\text{eff}}(q)$ the collective diffusion coefficient which can be experimentally determined by a short-time measurement of the dynamic structure factor $S(q, t) = \frac{1}{N} \sum_{i,j=1}^N \langle \exp(iq[r_i(0) - r_j(t)]) \rangle$. For small wavevectors $q \ll a^{-1}$ and $t < \tau$, with a being the mean particle distance and hydrodynamic interactions (HI) neglected or treated in a pair wise fashion, $S(q, t)$ is given by $S(q, t) = S(q, 0) \exp(-q^2 D^{\text{eff}}(q)t)$ [20]. Since $S(q, t=0)$ and $D_{\text{eff}}(q)$ can be experimentally determined from a short-time measurement, equation (3) predicts the long time behaviour of the MSD to be obtained already at short

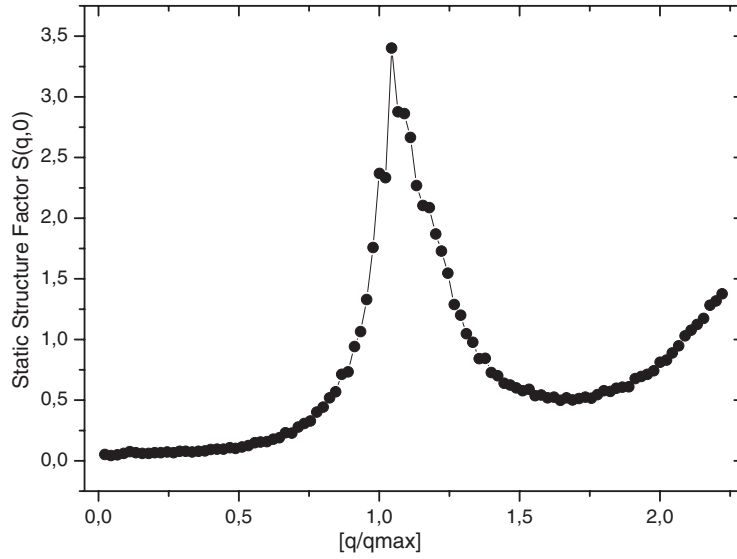


Figure 8. Real part of static structure factor $S(q, t = 0)$ for $\rho = 0.203 \mu\text{m}^{-1}$ ($q_{\text{max}} = 2\pi/a$).

times, i.e. significantly earlier than the crossover time from normal to SFD diffusion suggests (cf figure 5). To understand this—at first glance surprising—result, one has to realize that owing to the absence of mutual particle passages during SFD, the motion of a density wave with $q \ll a^{-1}$ is reflected by the trajectory of every individual particle. In contrast, when particles can pass each other, i.e. during normal diffusion, the motion of an arbitrarily chosen particle is decoupled from the collective motion of the system and equation (3) does not apply.

From the particle trajectories we determined the density dependent $S(q, t)$ for $t < 10$ s which is shown to be exemplarily for $q = 4q_{\text{min}}$ with $q_{\text{min}} = 1/R$ in the inset of figure 7 (owing to the finiteness of the system we are limited to wavevectors $q > q_{\text{min}} = 1/R$). From the vertical axis intercept and the slope we obtain $S(q, t = 0)$ and $D^{\text{eff}}(q)$ which allows us to calculate $F = \frac{S(q, 0)}{\rho} \sqrt{\frac{D^{\text{eff}}(q)}{\pi}}$ according to equation (3). The results are plotted for $3q_{\text{min}}$, $4q_{\text{min}}$, $5q_{\text{min}}$ and $6q_{\text{min}}$ as open symbols in figure 7 and show good agreement with the previously calculated values from the long-time MSD measurements (the deviations at small ρ are probably due to the breakdown of the long wave limit $q \ll a^{-1}$ of equation (3)). This result demonstrates the validity of equation (3) even in the case of finite systems as used here. This indicates that owing to the short-ranged electrostatic particle pair potential, particle correlations within the ring-shaped channels decay on a length scale much shorter than the perimeter of the system [21]. This is also seen by the behaviour of the static structure factor which is plotted in figure 8. The rather horizontal slope for $q \rightarrow 0$ resembles the behaviour of an infinite system and thus justifies *a posteriori* application of equation (3). In addition, this suggests that equation (3) is also valid in finite biological systems where the screening length is very small.

It should be emphasized that equation (3) is very general and applies for any other stochastic process in a many particle system as far as it remains translational invariant in space and time. In the absence of HI (and $q \rightarrow 0$), equation (3) simplifies to $\lim_{t \gg \tau} W(t) = \frac{1}{\rho} \sqrt{\frac{S(q)Dt}{\pi}}$ with D the diffusion constant of a single particle, i.e. $D = \text{const.}$

4. Conclusion

We have investigated the diffusion of colloidal particles in an optically created circular trap where the particles undergo SFD. Owing to the lack of sticking hydrodynamic conditions at the lateral confinement walls, this allows us to observe the transition from normal to SFD diffusion. In addition we compare the SFD mobility F obtained from long-time measurements of the MSD with the according values as obtained from a short-time measurement of the dynamic structure factor and find good agreement. Owing to the high flexibility of scanned optical tweezers one can also create channels with open ends which allow other particles to diffuse in and out. Such a situation is particularly interesting because it can serve as a model system for catalytic reactions in zeolitic materials which are important for a number of chemical processes [22].

Acknowledgments

We acknowledge helpful discussions with Ralf Bubeck. The work was financially supported from the Deutsche Forschungsgemeinschaft (Transregio SFB6).

References

- [1] Kollmann M 2003 *Phys. Rev. Lett.* **90** 180602
- [2] Gupta V, Nivarthi S S, McCormick A V and Davis H T 1995 *Chem. Phys. Lett.* **247** 596
- [3] Hahn K, Kärger J and Kukla V 1996 *Phys. Rev. Lett.* **76** 2762
- [4] Kukla V, Kornatowski J, Demuth D, Girmus I, Pfeifer H, Rees L V C, Schunk S, Unger K and Kärger J 1996 *Science* **272** 702
- [5] Levitt D G 1973 *Phys. Rev. A* **8** 3050
- [6] Kärger J 1992 *Phys. Rev. A* **45** 4173
- [7] Harris T E 1965 *J. Appl. Probab.* **2** 323
- [8] Jepsen D 1965 *J. Math. Phys.* **6** 405
- [9] van Beijeren H, Kehr K W and Kutner R 1983 *Phys. Rev. B* **28** 5711
- [10] Hahn K and Kärger J 1998 *J. Phys. Chem. B* **102** 5766
- [11] Jobic H, Hahn K, Kärger J, Bee M, Tuel A, Noack M, Girmus I and Kearley G J 1997 *J. Phys. Chem.* **110** 5834
- [12] Radhakrishnan R and Gubbins K E 1998 *Phys. Rev. Lett.* **79** 2847
- [13] Sholl D S and Fichthorn K A 1997 *Phys. Rev. Lett.* **79** 3569
- [14] Lin B, Cui B, Lee J-H and Yu J 2002 *Europhys. Lett.* **57** 724
- [15] Wei Q-H, Bechinger C and Leiderer P 2000 *Science* **287** 625
- [16] Palberg T, Härtl W, Wittig U, Versmold H, Würth M and Simnacher E 1992 *J. Phys. Chem.* **96** 8180
- [17] Ashkin A, Dziedzic J M, Bjorkholm J E and Chu S 1986 *Opt. Lett.* **11** 288
- [18] Faucheux L P, Stolovitzky G and Libchaber A 1995 *Phys. Rev. E* **51** 5239
- [19] Squires T M and Brenner M P 2000 *Phys. Rev. Lett.* **85** 4976
- [20] Nägele G 1996 *Phys. Rep.* **272** 215
- [21] Cui B, Diamant H and Lin B 2003 *Phys. Rev. Lett.* **89** 188302
- [22] Karpinski Z, Gandhi S N and Sachtler W M H 1993 *J. Catal.* **141** 337